VII International Conference on Computational Methods for Coupled Problems in Science and Engineering
COUPLED PROBLEMS 2017
M. Papadrakakis, E. Oñate and B. Schrefler (Eds)

MOTION OF A CYLINDER RIGID BODY INTERACTING WITH POINT VORTICES

Sokolov S. V.*

*Institute of Machines Science named after A.A.Blagonravov of the Russian Academy of Sciences (IMASH RAN) 4 Maly Kharitonyevsky Pereulok, Moscow 101990, RUSSIA
e-mail: sokolovsv72@mail.ru, web page: http://www.imash.ru/

Key words: point vortices, Hamiltonian systems, stability of equilibrium

Abstract. The dynamical behavior of a heavy circular cylinder and N point vortices in an ideal liquid is considered. The governing equations are presented in Hamiltonian form. Integrals of motion are found. Allowable types of trajectories are discussed. The stability of finding equilibrium solutions is investigated and some remarkable types of partial solutions of the system are presented. The system demonstrate chaotic behavior of dynamics.

1 INTRODUCTION

The problem of falling motion of a body in fluid has a long history and was considered in a series of the classical [7, 15] and modern papers [5, 10, 11, 12, 9, 8]. Some of the effects described in the papers, such as periodic rotation (tumbling), can be encountered only in viscous fluids.

The fluid's viscosity imposes resistive forces on the body. These forces manifest themselves not only through the skin friction but they also serve a source of vortex generation. To evaluate a model which is a more or less realistic and at the same time amenable to analytical treatment it is customary to assume the liquid to be ideal and add the vorticity *ad hoc* meaning that we postulate the existence of, say, circulation, point vortices or vortex sheets etc.

In previous works [14, 13] the problem of motion of the heavy cylinder under the action of gravity and a single point vortex was investigated with non-zero circulation.

In this paper we study the influence of the vorticity on the falling body in a trivial setting: a body (circular cylinder) subject to gravity is interacting dynamically with N point vortices. The circulation around the cylinder is not necessarily zero. So the model we consider here is exact and, at the same time, not so despairingly complex as most of the existing models are.

2 SETTING UP OF THE PROBLEM

Consider a circular cylinder subject to gravity moving in an unbounded volume of ideal liquid at rest at infinity. The cylinders element is orthogonal to the flow; thus the problem is essentially two-dimensional. There are N vortex filaments (point vortices) of strength Γ_i parallel to the cylinders element, here $i = \overline{1, N}$. The circulation Γ of the flow around the cylinder is, generally, different from zero (Fig. 1). Our goal is to detect and investigate the main features of the system.

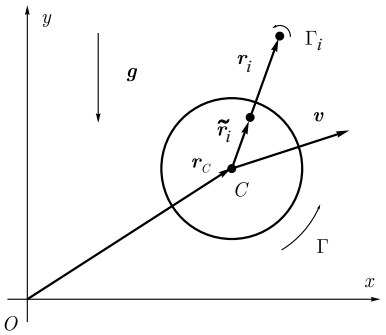

Figure 1: Circular cylinder and point vortices in the gravity field.

3 GOVERNING EQUATIONS

According to [13], the equations of motion for a cylinder and point vortices in the presence of gravity can be written as

$$\begin{aligned}
\dot{\boldsymbol{r}}_i &= -\boldsymbol{v} + \bigtriangledown \widetilde{\varphi}_i(\boldsymbol{r})|_{\boldsymbol{r}=\boldsymbol{r}_i}, \\
\dot{\boldsymbol{r}}_c &= \boldsymbol{v}, \\
a\dot{v}_1 &= \lambda v_2 - \sum_{i=1}^{N} \lambda_i(\dot{\widetilde{y}}_i - \dot{y}_i), \\
a\dot{v}_2 &= -\lambda v_1 + \sum_{i=1}^{N} \lambda_i(\dot{\widetilde{x}}_i - \dot{x}_i) - ag,
\end{aligned} \tag{1}$$

Here $\boldsymbol{r}_c = (x_c,\, y_c)$ is the radius-vector from the origin of a laboratory frame of reference Oxy to the cylinders center, $\boldsymbol{v} = (v_1,\, v_2)$ is the velocity of the cylinder, the radius-vector $\boldsymbol{r}_i = (x_i,\, y_i)$ is from the center of the cylinder to the i-th vortex, and $\widetilde{\boldsymbol{r}}_i = (\widetilde{x}_i,\, \widetilde{y}_i) = \frac{R^2 \boldsymbol{r}_i}{r_i^2}$ is the radius-vector from the center of the cylinder to the image of the i-th vortex (Fig. 1), R — the radius of the cylinder, the constant a is the mass plus the added mass of the cylinder, the constant ag is a gravity force applied to the cylinder, the constants λ and λ_i are related to the circulation and vortexs strength $\lambda = \frac{\Gamma}{2\pi}$, $\lambda_i = \frac{\Gamma_i}{2\pi}$. The density of the

fluid is assumed to be 2π. The function $\widetilde{\varphi}_i(\boldsymbol{r})$ represents that portion of the velocity potential $\varphi(\boldsymbol{r})$ which does not have a singularity at the point $\boldsymbol{r} = \boldsymbol{r}_i$:

$$\varphi(\boldsymbol{r}) = -\frac{R^2}{r^2}(\boldsymbol{r},\, \boldsymbol{v}) - \lambda \arctan\frac{y}{x} + \sum_{i=1}^{N} \lambda_i \left(\arctan\left(\frac{y-\widetilde{y}_i}{x-\widetilde{x}_i}\right) - \arctan\left(\frac{y-y_i}{x-x_i}\right)\right). \quad (2)$$

The equations (1) are similar to those from [13].

As in [13], one can note that the finite-dimensional system (1), which governs the motion of a cylinder and vortices in the gravity field, preserves the standard measure and can be represented in the Hamiltonian form.

Theorem 1. *The equations of motion* (1) *can be represented as follows:*

$$\dot{\zeta}_i = \{\zeta_i,\, H\} = \sum_k \{\zeta_i,\, \zeta_k\} \frac{\partial H}{\partial \zeta_k}, \quad (3)$$

where ζ_i *is the phase vector of the system* (1)*, that is,*

$$\zeta = \{x_1,\, y_1,\, \ldots,\, x_N,\, y_N,\, v_1,\, v_2,\, x_c,\, y_c\},$$

H is the Hamiltonian function, and the components of the skew-symmetric tensor of the Poisson structure $J_{ij}(\zeta) = \{\zeta_i,\, \zeta_j\}$ satisfy the Jacobi identity:

$$\sum_l \left(J_{il}\frac{\partial J_{jk}}{\partial \zeta_l} + J_{kl}\frac{\partial J_{ij}}{\partial \zeta_l} + J_{jl}\frac{\partial J_{ki}}{\partial \zeta_l}\right) = 0, \quad \forall i,\, j,\, k.$$

Proof. It is straightforward to check that the system (1) has a constant of motion which can be interpreted as the energy integral

$$H = \frac{1}{2}av^2 + \frac{1}{2}\sum_{i=1}^{N}\left(\lambda_i^2 \ln(r_i^2 - R^2) - \lambda_i\lambda \ln r_i^2\right) + \frac{1}{2}\sum_{i<j}\lambda_i\lambda_j \ln\frac{R^4 - 2R^2(\boldsymbol{r}_i,\, \boldsymbol{r}_j) + r_i^2 r_j^2}{|\boldsymbol{r}_i - \boldsymbol{r}_j|^2} + agy_c. \quad (4)$$

Assuming H be the Hamiltonian of our system, we now choose the components J_{ij} for the equations of motion (3) to be identical with the equations (1). The non-zero tensor components (as in [13]) read

$$\begin{gathered}
\{v_1,\, x_i\} = \frac{1}{a}\frac{r_i^4 - R^2(x_i^2 - y_i^2)}{r_i^4}, \quad \{v_1,\, y_i\} = -\frac{1}{a}\frac{2R^2 x_i y_i}{r_i^4}, \\
\{v_2,\, x_i\} = -\frac{1}{a}\frac{2R^2 x_i y_i}{r_i^4}, \quad \{v_2,\, y_i\} = \frac{1}{a}\frac{r_i^4 + R^2(x_i^2 - y_i^2)}{r_i^4}, \\
\{v_1,\, v_2\} = \frac{\lambda}{a^2} - \sum_{i=1}^{N}\frac{\lambda_i}{a^2}\frac{r_i^4 - R^4}{r_i^4}, \quad \{x_i,\, y_i\} = -\frac{1}{\lambda_i}, \\
\{x_c,\, v_1\} = \{y_c,\, v_2\} = \frac{1}{a}.
\end{gathered} \quad (5)$$

The check of the validity of the Jacoby identity for the components of (5) is a matter of straightforward computation. □

Thus, the fact that the equations (1) are Hamiltonian allows application of standard tools (e.g. for the stability analysis) from the extensively developed theory of Hamiltonian systems.

4 FIRST INTEGRALS AND REDUCTION

The presence of gravity breaks the rotational symmetry of the system, which implies the absence of an additional integral of motion which existed in the case $g = 0$. However, the system has two integrals of motion due to the translational symmetry: an autonomous integral P — projection of the systems linear momentum on the horizontal axis and a non-autonomous Q — projection of the systems linear momentum on the vertical axis:

$$\begin{aligned} Q &= a(v_2 + gt) + \lambda x_c - \sum_{i=1}^{N} \lambda_i(\widetilde{x}_i - x_i), \\ P &= av_1 - \lambda y_c + \sum_{i=1}^{N} \lambda_i(\widetilde{y}_i - y_i). \end{aligned} \tag{6}$$

Now we reduce the order of our system in the case $N = 1$. The system does not seem to have any additional constants of motion which is confirmed by chaotic behavior of solutions on the Poincaré section surface (Fig. 6, 7). A rigorous proof of non-itegrability of the system consisting of a body (with unequal added masses) with non-zero circulation around it falling in an ideal fluid is given in [2].

Using the autonomous integral P, one can reduce the original three-degree of freedom system to a system with two degrees of freedom.

To do this, put $P = 0$. It is clear that for $\lambda \neq 0$ (the case of $\lambda = 0$ will be addressed elsewhere) this can be always achieved by shifting the origin of the laboratory reference frame. Solving for y_c from the equation $P = 0$, substituting the result into the Hamiltonian (4) and excluding from (1) the equation in $\boldsymbol{r}_c$, we obtain the reduced system:

$$\begin{gathered} \dot{x}_1 = -v_1 + \left.\frac{\partial\widetilde{\varphi}}{\partial x}\right|_{\boldsymbol{r}=\overline{\boldsymbol{r}}_1}, \quad \dot{y}_1 = -v_2 + \left.\frac{\partial\widetilde{\varphi}}{\partial y}\right|_{\boldsymbol{r}=\overline{\boldsymbol{r}}_1}, \\ a\dot{v}_1 = \lambda v_2 - \lambda_1(\dot{\widetilde{y}}_1 - \dot{y}_1), \quad a\dot{v}_2 = -\lambda v_1 + \lambda_1(\dot{\widetilde{x}}_1 - \dot{x}_1) - ag \end{gathered} \tag{7}$$

which remains Hamiltonian with the Hamiltonian function

$$H_c = \frac{1}{2}av^2 + \frac{1}{2}\lambda_1^2 \ln(r_1^2 - R^2) - \frac{1}{2}\lambda_1\lambda \ln r_1^2 + \frac{ag}{\lambda}(av_1 + \lambda_1(\widetilde{y}_1 - y_1))$$

and the bracket structure obtained from (5) by eliminating the rows and columns corresponding to x_c and y_c.

5 CLASSIFICATION OF MOTIONS

Though our system is (comparatively) trivial, very few results concerned with the classification of the possible types of the cylinder and vortex trajectories can be obtained analytically. Numerical evidence show that there exist three types of motion (Fig. 2):

1) the cylinder and vortex are moving close to each other in a horizontal strip of finite width (Fig. 2a);
2) the cylinder "abandons" the vortex and then moves as in the previous case (Fig. 2b);
3) the cylinder "abandons" the vortex and travels down without bound ($y_c \to -\infty$) (Fig. 2c).

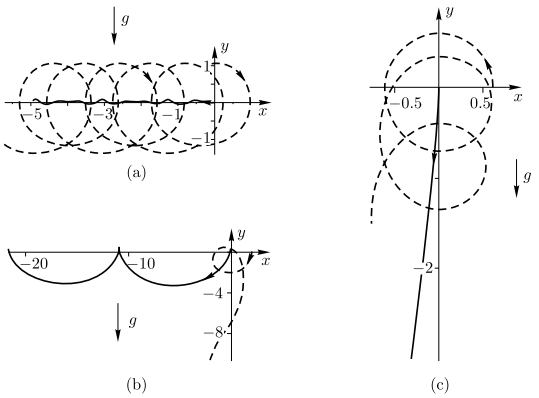

Figure 2: Motion of the cylinder (solid line) and the vortex (dashed line) in the field of gravity: (a) the cylinder and the vortex are moving in a bounded horizontal strip, the vortex is captured by the cylinder; (b) the cylinder moves in a bounded horizontal strip, the vortex is left behind; (c) the cylinder abandons the vortex and falls down without bound ($\lambda = \lambda_1$).

Thus, we have the capture of the vortex by the cylinder as in [4] and motion in a horizontal strip as described in [6].

So we hypothesize (but cannot prove it) that in the course of motion the cylinder is *always confined to a horizontal strip*, except, maybe, for the case $\lambda = \lambda_1$. If the cylinder falls down without bound (the function $y_c(t)$) tends to $-\infty$) the vortex cannot be captured with the cylinder.

6 RELATIVE EQUILIBRIA AND THEIR STABILITY

The stationary solutions of the reduced system (7) are the relative equilibria for the original system (1).

To find the equilibria we equate the right-hand sides of (7) to zero and thereby immediately obtain $v_2 = 0$, $v_1 = -\frac{ag}{\lambda}$. From hydrodynamical considerations it is clear that x_1 is necessarily zero meaning that the vortex and the cylinders center lie on the same vertical

line. (There are two other equilibria lying on the cylinders surface for which $x_1 \neq 0$; but this case is of little interest as the vortex merely annihilates with its image, so we will not consider it). Substituting the found x_1, v_1, and v_2 into the right-hand side of the first equation (7) yields

$$\overline{y}_1^4 + (\widetilde{\lambda}^2 - \widetilde{\lambda}\widetilde{\lambda}_1)\overline{y}_1^3 - \widetilde{\lambda}^2\overline{y}_1 - 1 = 0. \tag{8}$$

Here the following notation is used $\overline{y}_1 = \frac{y_1}{R}$, $\widetilde{\lambda} = \frac{\lambda}{\sqrt{agR}}$, $\widetilde{\lambda}_1 = \frac{\lambda_1}{\sqrt{agR}}$. It is interesting to note that a similar polynomial equation was obtained in [4] where advection of a point vortex in the field generated by an oscillating cylinder was studied.

Thus, the stationary solution of (7) is given by $(x_1,\, y_1,\, v_1,\, v_2) = \big(0,\, y_1,\, -\frac{ag}{\lambda},\, 0\big)$, where $y_1 = \overline{y}_1 R$ and $\overline{y}_1$ is a root of (8). For these solutions the cylinder and vortex are moving horizontally along parallel lines at a constant rate. For a hydrodynamically asymmetric body (the added masses are different) the stability of such rectilinear horizontal motions was investigated in [6].

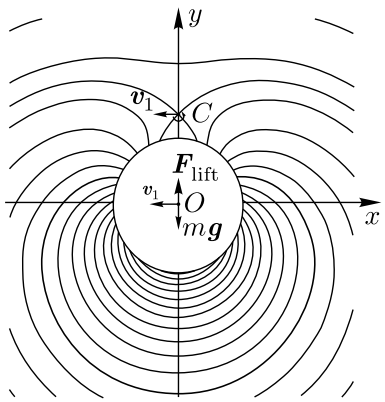

Figure 3: Cylinder and vortex in the state of relative equilibrium.

Physically, it is clear that for a cylinder to move with a constant speed the external forces applied to it must sum up to zero: the gravity must be compensated with the lift, which is due to the circulation. The vortex placed at the stagnation point C (Fig. 3) (at this point the velocity of the fluid particle relative to the cylinder is zero) does not move relative to the cylinder and therefore neither does its image. In this case the vortex exerts no force on the cylinder and therefore cannot prevent the cylinder from moving rectilinearly. The stream lines for this equilibrium case are depicted in Fig. 3.

It follows from (8) that the ordinate of the vortex relative equilibrium depends on the two parameters $\widetilde{\lambda}$ and $\widetilde{\lambda}_1$ (normalized circulation and vortex strength). For some value of $(\widetilde{\lambda},\, \widetilde{\lambda}_1)$ there are up to 4 equilibria (Fig. 4). Here an important restriction $|y_1| > R$ must be obeyed for the vortex to be outside the cylinder. Without loss of generality we assume $\widetilde{\lambda} > 0$. A schematic of the many-leaved surface (8) is given in Fig. 4. Consider the main features of the surface.

1. In the second quadrant of the plane $(\widetilde{\lambda}_1, \widetilde{\lambda})$, where $\widetilde{\lambda}_1 < 0$, $\widetilde{\lambda} > 0$, there is only one equilibrium below the cylinder (the lower leaf of the surface (8)).

2. In the first quadrant $(\widetilde{\lambda}_1 > 0, \widetilde{\lambda} > 0)$ there is an equilibrium above the cylinder (the upper leaf of the surface (8)). The lower leaf has a fold singularity, therefore, as indicted in Fig. 5, there may occur three equilibria: two below and one above the cylinder.

3. The upper leaf of (8) is truncated along the axis $\widetilde{\lambda}_1 = 0$ by the condition $y_1 > R$, meaning that the equilibria positions tend to the cylinders surface from above.

4. As in the previous case, the lower leaf and the fold stitched to it are truncated with the condition $y_1 < -R$ meaning that below the cylinder the equilibria exist in any small neighborhood of its surface.

5. Since (8) is unaltered under the transformation $\widetilde{\lambda}_1 \to -\widetilde{\lambda}_1$, $\widetilde{\lambda} \to -\widetilde{\lambda}$, it is clear that in the third and fourth quadrants the surface (8) can be constructed via rotation by 180° about the $\overline{y}_1$-axis of the surface from Fig. 4.

6. In Fig. 4 the stable equilibria defined by (8) dwell only on the intermediate leaf and are shown with dark-grey shading. The unstable equilibria form the entire upper and lower leaves (light-grey shading); the unstable equilibria on the intermediate leaf form the hatched region.

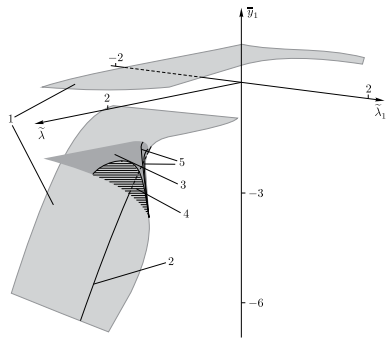

Figure 4: Equilibrium position $\overline{y}_1$ of the vortex depending on the parameters $\widetilde{\lambda}$, $\widetilde{\lambda}_1$: 1 — unstable equilibria ($ind = 1$), 2 — unstable equilibria (the form d^2H_c is degenerate, the instability can be deduced from the linearized equations), 3 — stable equilibria of the center-center type ($ind = 2$), 4 — unstable equilibria of the focus-focus type ($ind = 2$), 5 — resonance curves.

For the stability analysis of the equilibria found we will use the methods and approaches developed in [1]. It is well known that to investigate the stability of an equilibrium solution of a Hamiltonian system the two invariant characteristics of such a solution must be obtained:

1. the index of the quadratic form d^2H_c $\left(\text{i.e. the index of the symmetric } (4\times4)\text{-matrix } \left\|\frac{\partial^2 H_c}{\partial\zeta_k\,\partial\zeta_j}\right\|\right)$, which can vary from 0 to 4;
2. the type of the equilibrium solution depending on the eigenvalues of the linearized vector field $\left(\text{i. e. the eigenvalues of the symplectic } (4\times4)\text{-matrix } \left\|\sum_k J_{ik}\frac{\partial^2 H_c}{\partial\zeta_k\,\partial\zeta_j}\right\|\right)$. This type can be one of the following: center–center, saddle–center, saddle–saddle, focus–focus.

Like in [1], we mark off the eigenvalues of the linearized vector field, which are the roots of the characteristic polynomial

$$\chi(\mu) = \det\left(\sum_k J_{ik}\frac{\partial^2 H_c}{\partial\zeta_k\,\partial\zeta_j} - \mu E\right) = \mu^4 + a\mu^2 + b, \tag{9}$$

on the plane $(a,\ b)$ of the polynomial coefficients. In Fig. 5a from [1], one can see stable and unstable regions, the index of the form d^2H_c, and the types of the equilibrium solutions.

In Fig. 4, the upper and lower leaves are comprised of unstable solutions of the saddle–center type because here the index of d^2H_c is 1. These solutions correspond to the region $b<0$ in Fig. 5a. The points on the intermediate leaf (except for the resonance curves) are either unstable of the focus–focus type or stable of the center–center type; on this leaf the index of d^2H_c is 2.

Consider in greater detail the region in the first quadrant of the plane $(\widetilde{\lambda}_1,\ \widetilde{\lambda})$ where there are three equilibria. A close up of this part of the surface (8) is given in Fig. 5b. As in Fig. 4, the lower and upper leaves of the surface (8) represent unstable solutions with of the saddle–center type with $ind = 1$; the leaves correspond to the region $b<0$ in Fig. 5a. The intermediate leaf contains two types of points: stable (center-center) and unstable (focus–focus); everywhere on this leaf $ind = 2$. The stable solutions correspond to the region $\left(a>0,\ 0<b<\frac{a^2}{4}\right)$ in Fig. 5a. The unstable points form the region $b>\frac{a^2}{4}$. In Fig. 5a and Fig. 5b the third- and fourth-order resonances, defined by the equations $b=\frac{4a^2}{25}$ and $b=\frac{9a^2}{100}$, are shown. The resonances lie within the stable area. The analysis of the stability of the solutions on the boundaries $b=0$, $b=\frac{a^2}{4}$ and the resonance curves is not performed here as it entails a great amount of computation.

Finally, consider the equilibria corresponding to $\widetilde{\lambda}_1 = 2.1$ and $\widetilde{\lambda} = 4$. The Hill domains in the vicinity of these equilibria are depicted in Fig. 5c. The upper and lower equilibria are seen to be unstable and the intermediate one is stable.

Suppose that the circulation around the cylinder increases and the strength of the vortex is fixed. This can be imagined as if a vertical line moves along the $\widetilde{\lambda}$-axis in Fig. 5b. When this line crosses the boundary that corresponds to the parabola $b=\frac{a^2}{4}$ the type of the solution switches from center-center to focus-focus. The Hill domains in the vicinity

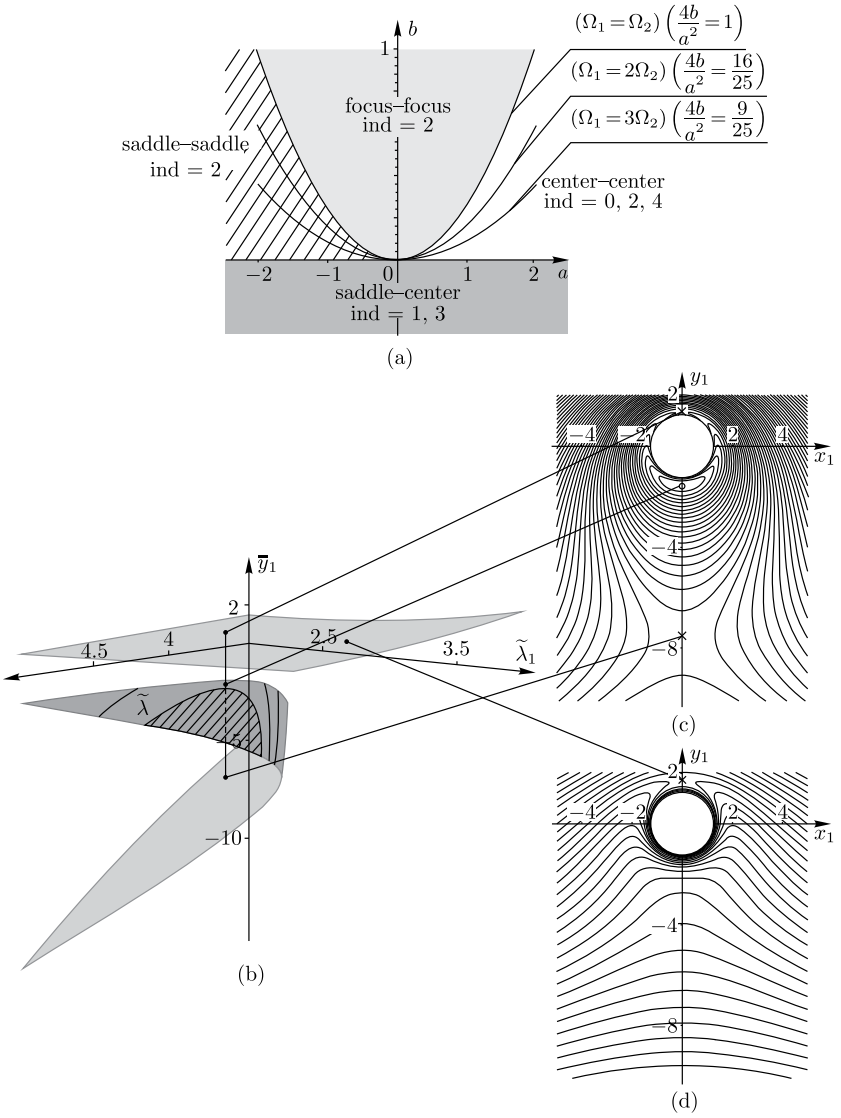

Figure 5: Equilibrium solutions and their stability. (a) Stable and unstable regions in the (a, b) plane of the characteristic polynomial coefficients. The third- and fourth-order resonance curves are shown. (b) The relative equilibrium position of the vortex versus the parameters $\widetilde{\lambda}$, $\widetilde{\lambda}_1$. Depending on the value of $\widetilde{\lambda}$, $\widetilde{\lambda}_1$ there can be a single equilibrium or even three equilibria. (c) The Hill domain for the three-equilibrium case. (d) The Hill domain for the single equilibrium case. In (c) and (d) the unstable equilibria are marked with crosses and the stable equilibria with circles.

of these solutions are analogous to those depicted in Fig. 5c. The intermediate solution becomes unstable.

Now let the circulation be fixed and the vortex strength grow. The imaginary vertical line moves along the $\widetilde{\lambda}_1$-axis. The stable center–center solution approaches the unstable focus–focus solution and they finally merge on the curve that corresponds to $b = 0$. As the vortex strength increases further there remains only one equilibrium (which is unstable) of the saddle–center type and located on the upper leaf (above the cylinder). The schematic of the Hill domain is given in Fig. 5d.

It should be noted that the boundaries that separate the stable solutions with $ind = 2$ from the unstable solutions with $ind = 2$ are very sensitive to the choice of the mass and radius of the cylinder a and R. At the same time, the surface (8) is independent of a and R. The type of the equilibria in Figs. 4 and 5 was determined for $a = 1,\ R = 1$.

7 POINCARÉ SECTION AND CHAOTIC BEHAVIOR OF THE DYNAMICAL SYSTEM

It is known that a system with insufficient number of conserved quantities (first integrals) is usually characterized with chaotic behavior of its trajectories. A strict proof of the property of non-integrability usually involves highly non-trivial mathematical argumentation. On the other hand, the chaotic dynamics of the system's solutions (that can be easily revealed via simulations) indicates the lack of first integrals.

Let us apply this line of reasoning to the system of equations (7), which is a Hamiltonian system with two degrees of freedom. To better understand its dynamics we plot a few Poincaré sections.

The phase vector of the system reads

$$\zeta = \{x_1,\, y_1,\, v_1,\, v_2,\}.$$

We fix $y_1 = 0.9$ thus picking a section plane in a neighborhood of the vortex's relative equilibrium. For $H_c = -17$ the Poincaré section is shown in Fig. 6. The other parameter's values $a = 1$, $R = 0.5$, $g = 10$, $\Gamma = 10$, $\Gamma_1 = 8.4375$.

In Fig. 6 points of the phase plane x_1v_1 which lie outside the region of allowable motion are shown with grey shading. We can see areas of regular dynamics which appear as intersection of the energy level surface and invariant tori. A stochastic layer is presented in the area surrounding second order tori. The appearance of this layer is a striking illustration of chaotic behavior of our system.

We can also build a Poincaré section on the energy level, which permits a spacial separation of points whose projections onto the plane x_1v_1 coincide. Section is depicted in Fig. 7.

In Fig. 7 we can also see regular and chaotic dynamics of the system for the given parameter values. The chaos is evidence of the absence of an additional integral of motion and confirm the hypothesis about non-integrability of our system. It seems to be curious to further explore the dynamics' evolution and possible scenarios of transition to

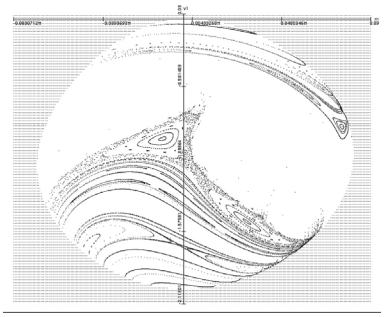

Figure 6: Poincaré section of the reduced cylinder-vortex system for $Hc = -17$; the system exhibits chaotic behavior.

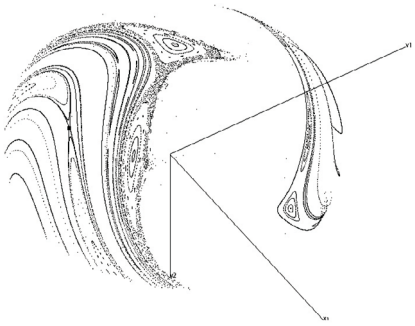

Figure 7: Poincaré section on the energy level $Hc = -17$ of the reduced cylinder-vortex system (the other parameter values are as those in Fig. 6). The small square marker indicates the position of the hyperbolic fixed point.

chaos. Poincaré sections of the reduced cylinder-vortex system are presented. The system exhibits chaotic behavior, which confirms the hypothesis [14, 13] about non-integrability of the system.

8 ACKNOWLEDGMENTS

This work is partially supported by the grants of RFBR No. 160100170, 160100809.

REFERENCES

[1] Bolsinov, A. V., Borisov, A. V., and Mamaev, I. S., The Bifurcation Analysis and the Conley Index in Mechanics, *Regul. Chaotic Dyn.*, 2012, vol. 17, no. 5, pp. 457–478.

[2] Borisov, A. V. and Mamaev, I. S., On the Motion of a Heavy Rigid Body in an Ideal Fluid with Circulation, *Chaos,* 2006, vol. 16, no. 1, 013118, 7 pp.

[3] Borisov, A. V., Ryabov, P. E., and Sokolov, S. V., Bifurcation analysis of the motion of a cylinder and a point vortex in an ideal fluid, *Mathematical Notes,* 2016, vol. 99, no. 5, pp 834–839

[4] Kadtke, J. B. and Novikov, E. A., Chaotic Capture of Vortices by a Moving Body: 1. The Single Point Vortex Case, *Chaos,* 1993, vol. 3, no. 4, pp. 543–553.

[5] Kozlov, V. V., On the Problem of Fall of a Rigid Body in a Resisting Medium, *Mosc. Univ. Mech. Bull.,* 1990, vol. 45, no. 1, pp. 30–36.

[6] Kozlov, V. V., On a Heavy Cylindrical Body Falling in a Fluid, *Izv. Ross. Akad. Nauk Mekh. Tverd. Tela,* 1993, no. 4, pp. 113–117 (Russian).

[7] Maxwell, J. K., On a Particular Case of Descent of a Heavy Body in a Resisting Medium, *Cambridge and Dublin Math. Journ.,* 1854, vol. 9, pp. 145–148.

[8] Sokolov S. V., Falling Motion of a Circular Cylinder Interacting Dynamically with N Point Vortices, *Rus. J. Nonlin. Dyn.,* 2014, vol. 10, no 1, pp. 59–72.

[9] Sokolov, S. V., Falling Motion of a Circular Cylinder Interacting Dynamically with a Vortex Pair in a Perfect Fluid, *Vestn. Udmurtsk. Univ. Mat. Mekh. Komp. Nauki,* 2014, no. 2, 86–99

[10] Sokolov, S. V., On the Problem of Falling Motion of a Circular Cylinder and a Vortex Pair in a Perfect Fluid, *Doklady Mathematics,* 2016, vol. 94, no. 2, pp. 594–597.

[11] Sokolov S. V., Koltsov I. S., Scattering of the Point Vortex by a Falling Circular Cylinder, *Doklady Physics,* 2015, vol. 60. no 11, pp. 511–514.

[12] Sokolov S. V., Koltsov I. S., Chaotic Scattering of the Point Vortex by Falling Circular Cylinder, *Vestn. Udmurtsk. Univ. Mat. Mekh. Komp. Nauki,* 2015, vol. 25, no 2, pp. 184–196.

[13] Sokolov S. V., Ramodanov S. M. Falling Motion of a Circular Cylinder Interacting Dynamically with a Point Vortex, *Reg. & Chaot. Dyn.,* 2013, vol. 18, no 1-2, p. 184–193.

[14] Sokolov S. V., Ramodanov S. M. Falling Motion of a Circular Cylinder Interacting Dynamically with a Point Vortex, *Rus. J. Nonlin. Dyn.,* 2012, vol. 8, no 3, pp. 617–628.

[15] Zhukovskii, N. E., On the Falling in the Air of Light Oblong Bodies Rotating About Their Longitudinal Axis, Paper I, *Collected Papers: Vol. 5,* Moscow–Leningrad: Gostekhizdat, 1937, pp. 72–80.